LSound - Theoretical background

Daniele Kempner Schultz and Eduardo Lenz Cardoso

September 30, 2024

1 Introduction

The linear partial differential equation for acoustics is [1]

$$\boldsymbol{\nabla} \cdot (\boldsymbol{\nabla} p(\mathbf{x}, t)) - \frac{1}{c^2}\left(\frac{\partial^2 p(\mathbf{x}, t)}{\partial t^2}\right) = 0, \quad \mathbf{x} \in \Omega, t \in [t_0, t_f] \tag{1}$$

where $p(\mathbf{x}, t)$ is pressure fluctuation around the mean value p_0, $\mathbf{x}$ are the coordinates of a point in the domain Ω, t is the time and c is the propagation velocity of the sound in the medium. This hyperbolic partial differential equation is known as the wave equation [2]. The analytical solution for this differential equation is known for some specific geometries, loads and boundary conditions, but complete solutions for general cases are hard to obtain without resorting to some numerical method [3].

Thus, this research aims to study the differential equation 1 and its solution by means of the Finite Element Method [4].

2 Finite Element Model

The complete solution for eq.(1) is the pressure $p(\mathbf{x}, t)$ that satisfies the differential equation for all $\mathbf{x} \in \Omega$ and for all t, along with the satisfaction of all boundary and initial conditions. Finding this function can be very hard for general Ω and boundary conditions [2]. Thus, one may aim for some form of approximation $\tilde{p}(\mathbf{x}, t)$. The weighted residual method [4] states that

$$\int_\Omega w(\mathbf{x}, t) \cdot r(\mathbf{x}, t)\, d\,\Omega = 0 \tag{2}$$

where

$$r(\mathbf{x}, t) = \boldsymbol{\nabla} \cdot (\boldsymbol{\nabla} \tilde{p}(\mathbf{x}, t)) - \frac{1}{c^2}\left(\frac{\partial^2 \tilde{p}(\mathbf{x}, t)}{\partial t^2}\right) \tag{3}$$

is the residual due to the approximate solution $\tilde{p}$ and w is a weight function. In this work, we assume that both $\tilde{p}$ and w respect the Dirichlet boundary conditions for all t. We also assume that both functions are written using the same set of base functions. In the Finite Element Method we start by defining a partition $\Omega_e \subseteq \Omega$ and a set of base functions $N(\mathbf{r})$ with compact support, such that

$$\tilde{p}(\mathbf{r}, t) = \sum_{i=1}^{n} N_i(\mathbf{r}) P_i(t) = \mathbf{N}(\mathbf{r})\mathbf{P}_e(t) \tag{4}$$

and

$$w(\mathbf{r},t) = \sum_{i=1}^{n} N_i(\mathbf{r}) W_i(t) = \mathbf{N}(\mathbf{r})\mathbf{W}_e(t) \tag{5}$$

where $\tilde{p}(\mathbf{r})$ and $w(\mathbf{r})$ are, respectively, the approximated pressure and weight inside Ω_e, as a function of the base functions N_i and discrete (nodal) values P_i and W_i at the n nodes of the element. It is assumed that the coordinates $\mathbf{r}$ inside Ω_e are defined in the range $[-1, 1]$. Matrix $\mathbf{N}$ is $1 \times n$ and vectors $\mathbf{P}_e$ and $\mathbf{W}_e$ are $n \times 1$. It is assumed that the base functions N_i are not function of time, such that

$$\frac{\partial^2 \tilde{p}(\mathbf{x},t)}{\partial t^2} = \mathbf{N}(\mathbf{r}) \frac{\partial^2 \mathbf{P}(t)_e}{\partial t^2} = \mathbf{N}(\mathbf{r}) \ddot{\mathbf{P}}_e(t). \tag{6}$$

Substituting eq.(3) into eq.(2) and integrating by parts with respect to the spatial coordinates results in

$$\int_\Gamma w \underbrace{(\boldsymbol{\nabla}\tilde{p} \cdot \boldsymbol{n})}_{p_n(t)} d\Gamma - \int_\Omega (\boldsymbol{\nabla} w) \cdot (\boldsymbol{\nabla}\tilde{p}) d\Omega - \frac{1}{c^2} \int_\Omega w \ddot{\tilde{p}} d\Omega = 0 \tag{7}$$

where $p_n(t)$ is the normal pressure on boundary Γ_e. Using the local interpolations and the fact that $\mathbf{W}_e(t)$, $\mathbf{P}_e(t)$ and $\ddot{\mathbf{P}}_e(t)$ do not depend on $\mathbf{r}$

$$\mathbf{W}_e^T \int_{\Gamma_e} \mathbf{N}^T p_n(t)\, d\,\Gamma_e - \mathbf{W}_e^T \int_{\Omega_e} \mathbf{B}^T \mathbf{B}\, d\,\Omega_e \mathbf{P}_e(t) - \mathbf{W}_e^T \frac{1}{c^2} \int_{\Omega_e} \mathbf{N}^T \mathbf{N}\, d\,\Omega_e \ddot{\mathbf{P}}_e(t) = 0 \tag{8}$$

where $\mathbf{B} = \boldsymbol{\nabla}\mathbf{N}$. Previous equation can be re-written as

$$\int_{\Gamma_e} \mathbf{N}^T p_n(t)\, d\,\Gamma_e - \int_{\Omega_e} \mathbf{B}^T \mathbf{B}\, d\,\Omega_e \mathbf{P}_e(t) - \frac{1}{c^2} \int_{\Omega_e} \mathbf{N}^T \mathbf{N}\, d\,\Omega_e \ddot{\mathbf{P}}_e(t) = \mathbf{0}. \tag{9}$$

The normal pressure on the boundary Γ_e, $p_n(t)$, can be associated to different sources. If the normal pressure is due to an imposed (known) normal velocity at the boundary (piston boundary condition), then

$$p_n(t) = -\rho \frac{dv_n(t)}{dt} \tag{10}$$

such that

$$\int_{\Gamma_e} \mathbf{N}^T p_n(t)\, d\,\Gamma_e = -\int_{\Gamma_e} \mathbf{N}^T \rho \frac{dv_n(t)}{dt}\, d\,\Gamma_e. \tag{11}$$

Other possibility is due to an absorbing boundary condition

$$p_n(t) = -Y_n \frac{dp(t)}{dt} \tag{12}$$

where Y_n is the admittance. In such case

$$\int_{\Gamma_e} \mathbf{N}^T p_n(t)\, d\,\Gamma_e = -\int_{\Gamma_e} \mathbf{N}^T Y_n \mathbf{N} \dot{\mathbf{P}}_e\, d\,\Gamma_e. \tag{13}$$

Thus, one obtain

$$\underbrace{\int_{\Omega_e} \mathbf{B}^T \mathbf{B}\, d\,\Omega_e}_{\mathbf{K}_e} \mathbf{P}_e(t) + \underbrace{Y_n \int_{\Gamma_e} \mathbf{N}^T \mathbf{N}\, d\,\Gamma_e}_{\mathbf{C}_e} \dot{\mathbf{P}}_e + \underbrace{\frac{1}{c^2} \int_{\Omega_e} \mathbf{N}^T \mathbf{N}\, d\,\Omega_e}_{\mathbf{M}_e} \ddot{\mathbf{P}}_e(t) = \underbrace{\rho \int_{\Gamma_e} \mathbf{N}^T \frac{dv_n(t)}{dt}\, d\,\Gamma_e}_{\mathbf{F}_e(t)}. \tag{14}$$

As the base functions have compact support and assuming non overlapping elements, it is possible to represent the original domain Ω as a superposition of the individual elements Ω_e as

$$\mathbf{K}\mathbf{P}(t) + \mathbf{C}\dot{\mathbf{P}}(t) + \mathbf{M}\ddot{\mathbf{P}}(t) = \mathbf{F}(t) \tag{15}$$

where

$$\mathbf{K} = \sum_{e=1}^{n_e} \mathbf{H}_e^T \mathbf{K}_e \mathbf{H}_e, \quad \mathbf{M} = \sum_{e=1}^{n_e} \mathbf{H}_e^T \mathbf{M}_e \mathbf{H}_e, \quad \mathbf{C} = \sum_{e=1}^{n_e} \mathbf{H}_e^T \mathbf{C}_e \mathbf{H}_e, \tag{16}$$

and

$$\mathbf{F}(t) = \sum_{e=1}^{n_e} \mathbf{H}_e^T \mathbf{F}_e(t) \tag{17}$$

are, respectively, the global stiffness matrix, the global inertia matrix and the global source vector. Matrices $\mathbf{K}$, $\mathbf{C}$ and $\mathbf{M}$ are $n_{tot} \times n_{tot}$, where n_{tot} is the number of nodes in Ω. Vectors $\mathbf{P}$ and $\mathbf{F}$ are the global vector of nodal pressures and the global loading vector, both with dimension $n_{tot} \times 1$. $\mathbf{H}_e$ is an $n \times n_{tot}$ localization matrix. Equation 15 is a linear system of Ordinary Differential Equations, where the time t is the independent variable.

In the following we investigate the particularization of the previous equations to three and two dimensional models. In particular, we use the four node bilinear isoparametric element as reference for the bidimensional implementation and the eigth node trilinear isoparametric elements as references for the three dimensional case.

3 Bidimensional Elements

Bidimensional elements are defined in a 2D domain $\Omega(x, y)$ with elements defined in a normalized domain $\Omega_e(r, s)$ with $r \in [-1, 1]$ and $s \in [-1, 1]$, as shown in Fig. 1.

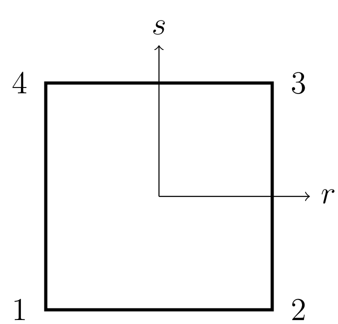

Figure 1: Geometry and node numbers for the bilinear isoparametric element.

Matrix $\mathbf{B}(r, s) = \boldsymbol{\nabla}\mathbf{N}(r, s)$ is particularized to

$$\mathbf{B}(r, s) = \begin{bmatrix} \frac{dN_1(r,s)}{dx} & \cdots & \frac{dN_n(r,s)}{dx} \\ \frac{dN_1(r,s)}{dy} & \cdots & \frac{dN_n(r,s)}{dy} \end{bmatrix} \tag{18}$$

where, for isoparametric elements,

$$\mathbf{J}(r, s) = \begin{bmatrix} \sum_{i=1}^{n} \frac{dN_i}{dr} X_i & \sum_{i=1}^{n} \frac{dN_i}{dr} Y_i \\ \sum_{i=1}^{n} \frac{dN_i}{ds} X_i & \sum_{i=1}^{n} \frac{dN_i}{ds} Y_i \end{bmatrix} \tag{19}$$

is the Jacobian matrix at r, s such that

$$dxdy = |\mathbf{J}(r,s)|drds. \tag{20}$$

The bilinear isoparametric element has four nodes ($n = 4$) and the shape functions are

$$N_1(r,s) = \frac{1}{4}(1-r)(1-s) \tag{21}$$

$$N_2(r,s) = \frac{1}{4}(1+r)(1-s) \tag{22}$$

$$N_3(r,s) = \frac{1}{4}(1+r)(1+s) \tag{23}$$

$$N_4(r,s) = \frac{1}{4}(1-r)(1+s) \tag{24}$$

The edges for this element are defined as

1. nodes 1 and 2 ($s = -1$)
2. nodes 2 and 3 ($r = 1$)
3. nodes 4 and 3 ($s = 1$)
4. nodes 4 and 1 ($r = -1$)

Integrals defined on the edges ($r = \pm 1$ or $s = \pm 1$) of this element are defined in the next subsections.

3.1 Edge with $s = \pm 1$

In this case, the (isoparametric) differential mappings are

$$\frac{dx}{dr} = \sum_{i=1}^{n} \frac{dN_i(r, \pm 1)}{dr} X_i \tag{25}$$

and

$$\frac{dy}{dr} = \sum_{i=1}^{n} \frac{dN_i(r, \pm 1)}{dr} Y_i \tag{26}$$

such that

$$d\mathbf{t}(r, \pm 1) = \begin{Bmatrix} \frac{dx}{dr} \\ \frac{dy}{dr} \end{Bmatrix} \tag{27}$$

is the tangent vector to the edge, with magnitude

$$||d\mathbf{t}(r, \pm 1)||dr = d\mathbf{x}. \tag{28}$$

3.2 Edge with $r = \pm 1$

In this case, the (isoparametric) differential mappings are

$$\frac{dx}{ds} = \sum_{i=1}^{n} \frac{dN_i(\pm 1, s)}{ds} X_i \tag{29}$$

and

$$\frac{dy}{ds} = \sum_{i=1}^{n} \frac{dN_i(\pm 1, s)}{ds} Y_i \tag{30}$$

such that

$$d\mathbf{t}(\pm 1, s) = \begin{Bmatrix} \frac{dx}{ds} \\ \frac{dy}{ds} \end{Bmatrix} \tag{31}$$

is the tangent vector to the edge, with magnitude

$$||d\mathbf{t}(\pm 1, s)||ds = d\mathbf{x}. \tag{32}$$

3.3 Particularization for the triangular element

The triangular element can be obtained from the bilinear element if we collapse nodes 3 and 4, as shown in Fig. 2.

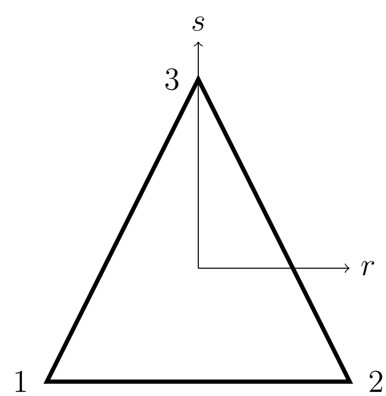

Figure 2: Geometry and node numbers for the triangular element.

In such case, the resulting shape functions are

$$N_1(r, s) = \frac{(r-1)s - r + 1}{4} \tag{33}$$

$$N_2(r, s) = -\frac{(r+1)s - r - 1}{4} \tag{34}$$

$$N_3(r, s) = \frac{1}{2}(s+1) \tag{35}$$

and there are only three edges: bottom ($s = -1$), right ($r = 1$) and left ($r = -1$).

Thus, edges for triangular elements are defined as

1. nodes 1 and 2 ($s = -1$)

2. nodes 2 and 3 ($r = 1$)

3. nodes 3 and 1 ($r = -1$)

For this element, matrix $\mathbf{B}$ can be written as

$$\mathbf{B} = \frac{1}{\Delta} \begin{bmatrix} y_{23} & y_{31} & y_{12} \\ x_{32} & x_{13} & x_{21} \end{bmatrix} \tag{36}$$

in which $y_{23} = y_2 - y_3$, for example, and

$$\Delta = x_{21}y_3 + x_{13}y_2 + x_{32}y_1. \tag{37}$$

As matrix $\mathbf{B}$ is not a function of the coordinates inside Ω_e, it follows that the stiffness matrix can be evaluated as

$$\int_{\Omega_e} \mathbf{B}^T\mathbf{B} d\Omega_e = \mathbf{B}^T\mathbf{B} \int_{\Omega_e} d\Omega_e = \mathbf{B}^T\mathbf{B} A_e \tag{38}$$

in which

$$A_e = \frac{1}{2} \begin{vmatrix} 1 & x_1 & y_1 \\ 1 & x_2 & y_2 \\ 1 & x_3 & y_3 \end{vmatrix} \tag{39}$$

is the area of the triangle.

4 Tridimensional Elements

Tridimensional elements are defined in a 3D domain $\Omega(x, y, z)$ with elements defined in a normalized domain $\Omega_e(r, s, t)$ with $r \in [-1, 1]$, $s \in [-1, 1]$ and $t \in [-1, 1]$, as shown in Fig 3.

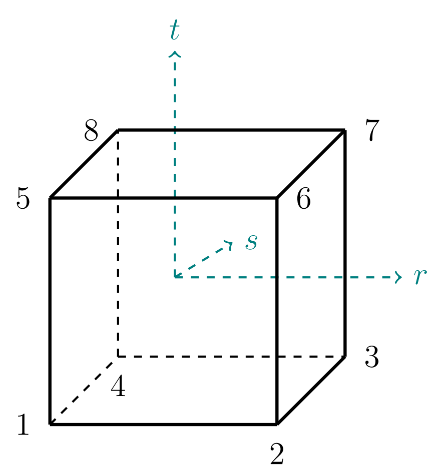

Figure 3: Geometry and node numbers for the trilenear hexaedrical element.

Matrix $\mathbf{B}(r, s, t) = \boldsymbol{\nabla}\mathbf{N}(r, s, t)$ is particularized to

$$\mathbf{B}(r, s, t) = \begin{bmatrix} \frac{dN_1(r,s,t)}{dx} & \dots & \frac{dN_n(r,s,t)}{dx} \\ \frac{dN_1(r,s,t)}{dy} & \dots & \frac{dN_n(r,s,t)}{dy} \\ \frac{dN_1(r,s,t)}{dz} & \dots & \frac{dN_n(r,s,t)}{dz} \end{bmatrix} \tag{40}$$

where, for isoparametric elements,

$$\mathbf{J}(r,s,t) = \begin{bmatrix} \sum_{i=1}^{n} \frac{dN_i}{dr} X_i & \sum_{i=1}^{n} \frac{dN_i}{dr} Y_i & \sum_{i=1}^{n} \frac{dN_i}{dr} Z_i \\ \sum_{i=1}^{n} \frac{dN_i}{ds} X_i & \sum_{i=1}^{n} \frac{dN_i}{ds} Y_i & \sum_{i=1}^{n} \frac{dN_i}{ds} Z_i \\ \sum_{i=1}^{n} \frac{dN_i}{dt} X_i & \sum_{i=1}^{n} \frac{dN_i}{dt} Y_i & \sum_{i=1}^{n} \frac{dN_i}{dt} Z_i \end{bmatrix} \tag{41}$$

is the Jacobian matrix at r, s such that

$$dxdydz = |\mathbf{J}(r,s,t)|drdsdt. \tag{42}$$

The trilinear isoparametric element has eight nodes ($n = 8$) and the following shape functions

$$N_1(r,s,t) = \frac{1}{8}(1-r)(1-s)(1-t) \tag{43}$$

$$N_2(r,s,t) = \frac{1}{8}(1+r)(1-s)(1-t) \tag{44}$$

$$N_3(r,s,t) = \frac{1}{8}(1+r)(1+s)(1-t) \tag{45}$$

$$N_4(r,s,t) = \frac{1}{8}(1-r)(1+s)(1-t) \tag{46}$$

$$N_5(r,s,t) = \frac{1}{8}(1-r)(1-s)(1+t) \tag{47}$$

$$N_6(r,s,t) = \frac{1}{8}(1+r)(1-s)(1+t) \tag{48}$$

$$N_7(r,s,t) = \frac{1}{8}(1+r)(1+s)(1+t) \tag{49}$$

$$N_8(r,s,t) = \frac{1}{8}(1-r)(1+s)(1+t) \tag{50}$$

The faces for this element are defined as

1. nodes 1234 ($t = -1$)
2. nodes 5678 ($t = 1$)
3. nodes 1265 ($s = -1$)
4. nodes 2376 ($r = 1$)
5. nodes 4378 ($s = 1$)
6. nodes 1485 ($r = -1$)

Integrals defined on the faces of this element ($r = \pm 1$ or $s = \pm 1$ or $t = \pm 1$) are defined in the following.

4.0.1 Faces with $t = \pm 1$

This is the situation for the faces defined by nodes 1234 ($t = -1$) and 5678 ($t = 1$).

In this case, the (isoparametric) differential mappings are

$$\frac{dx}{dr} = \sum_{i=1}^{n} \frac{dN_i(r,s,\pm 1)}{dr} X_i \quad \frac{dx}{ds} = \sum_{i=1}^{n} \frac{dN_i(r,s,\pm 1)}{ds} X_i \tag{51}$$

$$\frac{dy}{dr} = \sum_{i=1}^{n} \frac{dN_i(r,s,\pm 1)}{dr} Y_i \quad \frac{dy}{ds} = \sum_{i=1}^{n} \frac{dN_i(r,s,\pm 1)}{ds} Y_i \tag{52}$$

$$\frac{dz}{dr} = \sum_{i=1}^{n} \frac{dN_i(r,s,\pm 1)}{dr} Z_i \quad \frac{dz}{ds} = \sum_{i=1}^{n} \frac{dN_i(r,s,\pm 1)}{ds} Z_i \tag{53}$$

such that we can define two tangents

$$d\mathbf{t}_1(r,s,\pm 1) = \begin{Bmatrix} \frac{dx}{dr} \\ \frac{dy}{dr} \\ \frac{dz}{dr} \end{Bmatrix} = \mathbf{J}_1^T \tag{54}$$

and

$$d\mathbf{t}_2(r,s,\pm 1) = \begin{Bmatrix} \frac{dx}{ds} \\ \frac{dy}{ds} \\ \frac{dz}{ds} \end{Bmatrix} = \mathbf{J}_2^T, \tag{55}$$

where $\mathbf{J}_i$ is the i-th row of $\mathbf{J}$.

The normal to this two tangent vectors is the area differential

$$d\mathbf{n} = d\mathbf{t}_1 \times d\mathbf{t}_2 \tag{56}$$

such that

$$dxdydz = ||d\mathbf{n}||drds. \tag{57}$$

4.0.2 Faces with $r = \pm 1$

This is the situation for the faces defined by nodes 2376 ($r = 1$) and 1485 ($r = -1$).

In this case, the (isoparametric) differential mappings are

$$\frac{dx}{ds} = \sum_{i=1}^{n} \frac{dN_i(\pm 1,s,t)}{ds} X_i \quad \frac{dx}{dt} = \sum_{i=1}^{n} \frac{dN_i(\pm 1,s,t)}{dt} X_i \tag{58}$$

$$\frac{dy}{ds} = \sum_{i=1}^{n} \frac{dN_i(\pm 1,s,t)}{ds} Y_i \quad \frac{dy}{dt} = \sum_{i=1}^{n} \frac{dN_i(\pm 1,s,t)}{dt} Y_i \tag{59}$$

$$\frac{dz}{ds} = \sum_{i=1}^{n} \frac{dN_i(\pm 1,s,t)}{ds} Z_i \quad \frac{dz}{dt} = \sum_{i=1}^{n} \frac{dN_i(\pm 1,s,t)}{dt} Z_i \tag{60}$$

such that we can define two tangents

$$d\mathbf{t}_1(\pm 1,s,t) = \begin{Bmatrix} \frac{dx}{ds} \\ \frac{dy}{ds} \\ \frac{dz}{ds} \end{Bmatrix} = \mathbf{J}_2^T \tag{61}$$

and

$$d\mathbf{t}_2(\pm 1,s,t) = \begin{Bmatrix} \frac{dx}{dt} \\ \frac{dy}{dt} \\ \frac{dz}{dt} \end{Bmatrix} = \mathbf{J}_3^T. \tag{62}$$

The normal to this two tangent vectors is the area differential

$$d\mathbf{n} = d\mathbf{t}_1 \times d\mathbf{t}_2 \tag{63}$$

such that

$$dxdydz = ||d\mathbf{n}||dsdt. \tag{64}$$

4.0.3 Faces with $s = \pm 1$

This is the situation for the faces defined by nodes 1265 ($s = -1$) and 4378 ($s = 1$).

In this case, the (isoparametric) differential mappings are

$$\frac{dx}{dr} = \sum_{i=1}^{n} \frac{dN_i(r, \pm 1, t)}{dr} X_i \quad \frac{dx}{dt} = \sum_{i=1}^{n} \frac{dN_i(r, \pm 1, t)}{dt} X_i \tag{65}$$

$$\frac{dy}{dr} = \sum_{i=1}^{n} \frac{dN_i(r, \pm 1, t)}{dr} Y_i \quad \frac{dy}{dt} = \sum_{i=1}^{n} \frac{dN_i(r, \pm 1, t)}{dt} Y_i \tag{66}$$

$$\frac{dz}{dr} = \sum_{i=1}^{n} \frac{dN_i(r, \pm 1, t)}{dr} Z_i \quad \frac{dz}{dt} = \sum_{i=1}^{n} \frac{dN_i(r, \pm 1, t)}{dt} Z_i \tag{67}$$

such that we can define two tangents

$$d\mathbf{t}_1(\pm 1, s, t) = \begin{Bmatrix} \frac{dx}{dr} \\ \frac{dy}{dr} \\ \frac{dz}{dr} \end{Bmatrix} = \mathbf{J}_1^T \tag{68}$$

and

$$d\mathbf{t}_2(\pm 1, s, t) = \begin{Bmatrix} \frac{dx}{dt} \\ \frac{dy}{dt} \\ \frac{dz}{dt} \end{Bmatrix} = \mathbf{J}_3^T. \tag{69}$$

The normal to this two tangent vectors is the area differential

$$d\mathbf{n} = d\mathbf{t}_1 \times d\mathbf{t}_2 \tag{70}$$

such that

$$dxdydz = ||d\mathbf{n}||drdt. \tag{71}$$

4.1 Particularization for thetraedra

If we collapse nodes 3 and 4 into 3 and also nodes 5, 6, 7 and 8 into a new node 4, this will result in the 4 faces of the element as shown in Fig. 4.

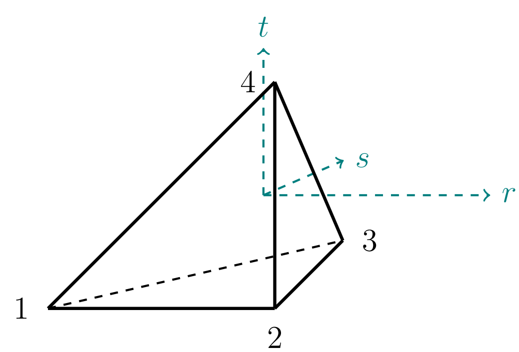

Figure 4: Geometry and node numbers for the tetra element.

In this case the shape functions are

$$N_1(r,s,t) = -\frac{((r-1)s-r+1)t+(1-r)s+r-1}{8} \tag{72}$$

$$N_2(r,s,t) = \frac{((r+1)s-r-1)t+(-r-1)s+r+1}{8} \tag{73}$$

$$N_3(r,s,t) = -\frac{((s+1)t-s-1}{4} \tag{74}$$

$$N_4(r,s,t) = \frac{1}{2}(t+1) \tag{75}$$

Faces for this element are defined as

1. 123 ($t = -1$)
2. 234 ($r = 1$)
3. 134 ($r = -1$)

As matrix $\mathbf{B}$ is not a function of the coordinates inside Ω_e, it follows that the stiffness matrix can be evaluated as

$$\int_{\Omega_e} \mathbf{B}^T\mathbf{B}d\Omega_e = \mathbf{B}^T\mathbf{B}\int_{\Omega_e} d\Omega_e = \mathbf{B}^T\mathbf{B}V_e \tag{76}$$

in which

$$V_e = \frac{1}{6}\begin{vmatrix} x_1 & y_1 & z_1 \\ x_2 & y_2 & z_2 \\ x_3 & y_3 & z_3 \end{vmatrix} \tag{77}$$

is the volume of the tetrahedron.

4.2 Particularization for pyramid

If we collapse nodes nodes 5, 6, 7 and 8 into a new node 5, this will result in the 5 faces of the element, as shown in Fig. 5.

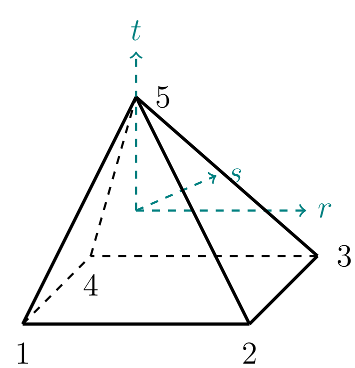

Figure 5: Geometry and node numbers for the pyramidal element.

In this case the shape functions are

$$N_1(r,s,t) = -\frac{[(r-1)s-r+1]\,t+(1-r)s+r-1}{8} \tag{78}$$

$$N_2(r,s,t) = \frac{[(r+1)s-r-1]\,t+(-r-1)s+r+1}{8} \tag{79}$$

$$N_3(r,s,t) = -\frac{[(r+1)s+r+1]\,t+(-r-1)s-r-1}{8} \tag{80}$$

$$N_4(r,s,t) = \frac{((r-1)s+r-1)\,t+(1-r)s-r+1}{8} \tag{81}$$

$$N_5(r,s,t) = \frac{1}{2}(t+1) \tag{82}$$

Faces for this element are defined as

1. 1234 ($t=-1$)
2. 125 ($s=-1$)
3. 235 ($r=1$)
4. 345 ($s=1$)
5. 415 ($r=-1$)

Local matrices for this element follow the same procedure used in the Trilinear element, but for this restricted set of shape functions and nodes.

References

[1] F. Jacobsen and P.M. Juhl. *Fundamentals of General Linear Acoustics*. Wiley, 2013.

[2] S.J. Farlow. *Partial Differential Equations for Scientists and Engineers*. Dover Books on Mathematics. Dover Publications, 2012.

[3] Albert G Prinn. A review of finite element methods for room acoustics. In *Acoustics*, volume 5, pages 367–395. MDPI, 2023.

[4] Thomas J.R Hughes. *Finite element method:linear static and dynamic finite element analysis*. Prentice Hall, Englewood Cliffs, 1987.